The human hippocampus contributes to both the recollection and familiarity components of recognition memory

Maxwell B. Merkow[a,1], John F. Burke[b], and Michael J. Kahana[c]

[a]Department of Neurosurgery, University of Pennsylvania, Philadelphia, PA 19104; [b]Perelman School of Medicine, University of Pennsylvania, Philadelphia, PA 19104; and [c]Department of Psychology, University of Pennsylvania, Philadelphia, PA 19104

Edited by Larry R. Squire, Veterans Affairs San Diego Healthcare System, San Diego, CA, and approved September 30, 2015 (received for review July 31, 2015)

Despite a substantial body of work comprising theoretical modeling, the effects of medial temporal lobe lesions, and electrophysiological signal analysis, the role of the hippocampus in recognition memory remains controversial. In particular, it is not known whether the hippocampus exclusively supports recollection or both recollection and familiarity—the two latent cognitive processes theorized to underlie recognition memory. We studied recognition memory in a large group of patients undergoing intracranial electroencephalographic (iEEG) monitoring for epilepsy. By measuring high-frequency activity (HFA)—a signal associated with precise spatiotemporal properties—we show that hippocampal activity during recognition predicted recognition memory performance and tracked both recollection and familiarity. Through the lens of dual-process models, these results indicate that the hippocampus supports both the recollection and familiarity processes.

hippocampus | recognition memory | recollection | familiarity | high-frequency activity

Recognition is one's ability to judge an item as previously encountered. Whereas it is well known that the hippocampus plays a crucial role in human recall memory, the role of the hippocampus in recognition memory remains surprisingly controversial (1–4). A number of studies have reported that bilateral hippocampal injury in humans causes impaired recall, whereas recognition remains intact (5). Others document the preservation of recognition in the setting of hippocampal lesioning in nonhuman primates (6) and rodents (7). On the other hand, a substantial literature describes combined recall and recognition deficits in a similarly injured group of patients (8) and animals (9, 10).

Recognition is thought to rely on two processes: familiarity, wherein upon seeing a person's face, the rememberer has only a vague sense he has met the person before, and recollection, wherein the subject sees the person's face and vividly remembers details of the encounter (11, 12). What role the hippocampus plays in supporting these processes remains the subject of considerable debate. Many memory researchers have proposed the discrepancy in the lesion data above derives from the fact that the hippocampus, which is well known to play a role in associative and relational memory (13), exclusively subserves recollection, whereas familiarity is supported by the extrahippocampal medial temporal lobe (MTL) (14). By this account, humans and animals are able to compensate for the loss of the hippocampus, and thus recollection, by relying on familiarity (15–18). A contrasting view holds that the hippocampus instead contributes to both recollection and familiarity, thus explaining why hippocampal damage is associated with severe impairment of both processes and consequently the overall recognition performance (4, 8, 19, 20). Whether neural circuitry underlying familiarity and recollection lie within the hippocampus has also been extensively studied using functional MRI (fMRI) (21). Still, that many fMRI experiments show that only recollection signals are found in the hippocampus (22–24) whereas others report blood oxygen level-dependent signal representing both recollection and familiarity in this structure (25), further fuels the debate regarding which aspects of recognition memory are supported by the hippocampus. Although many electrophysiology studies demonstrate neural dissociations in the hippocampus during recognition (24, 26–29), they do not answer the question whether this structure subserves solely recollection or both recollection and familiarity.

In this study, we used intracranially recorded high-frequency activity (HFA) to elucidate the role of the human hippocampus in recognition memory. Given that HFA is a spatiotemporally precise marker of neural ensemble activity (30, 31), if hippocampal activity correlated with successful recognition performance at retrieval, then, depending on which theory is correct, it should correlate either with behavioral estimates of recollection only or with behavioral estimates of both recollection and familiarity. Seen through the lens of dual-process theories of recognition (12), hippocampal HFA should identify whether this structure uniquely supports recollection. We tested these hypotheses in a group of 66 epilepsy patients undergoing intracranial monitoring to assess the specific role of the hippocampus in recognition memory.

Results

We analyzed the behavioral and neural data from 66 (24 female) left-language–dominant epilepsy patients (mean age, 33.8) during an item recognition memory task (Fig. S1*A*) consisting of stimuli (targets or lures) and subject response choices (old and new). The subject's goal was to correctly match his/her response choice

Significance

Recognition memory is thought to be composed of recollection, accompanied by vivid details, and familiarity or a general sense of knowing. A fundamental and long-standing question remains: Which of these processes does the hippocampus support? We measured high-frequency activity (HFA), a spatiotemporally precise signal of neural activation, in subjects undergoing direct brain recordings and found that hippocampal HFA dissociated based on both the stimulus evidence presented and the response choice. Hippocampal HFA predicted overall memory performance as well as individual differences in both recollection and familiarity estimates. Our findings reject the hypothesis that the hippocampus exclusively supports the recollection component of recognition memory and, instead, indicate that this structure is functionally relevant to both processes thought to support recognition.

Author contributions: M.B.M. and M.J.K. designed research; M.B.M. performed research; M.B.M. and J.F.B. analyzed data; and M.B.M., J.F.B., and M.J.K. wrote the paper.

The authors declare no conflict of interest.

This article is a PNAS Direct Submission.

[1]To whom correspondence should be addressed. Email: maxwell.merkow@uphs.upenn.edu.

This article contains supporting information online at www.pnas.org/lookup/suppl/doi:10.1073/pnas.1513145112/-/DCSupplemental.

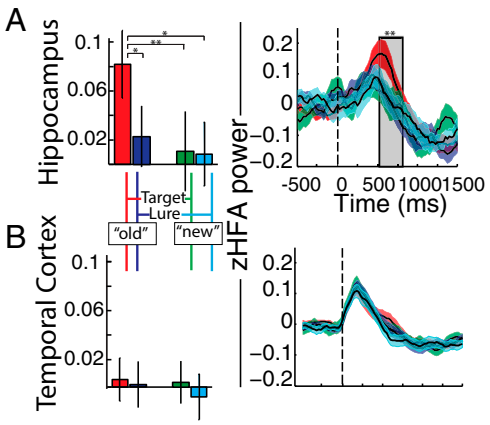

Fig. 1. (*A*) *z*HFA in the hippocampus during recognition. The left panel displays mean and ±1 SEM of subjects' *z*HFA during recognition based on target–lure status and response choice (old, new) factors during the 200–1,000 ms following presentation of a test item. *z*HFA did not significantly vary as function or target–lure status nor response choice; however, there was a significant interaction between these two factors. *z*HFA associated with hit (true-positive) trials was greater than the other three types of trials. The panel displays *z*HFA values for each target–lure and response choice combination (color schema same as in *A*) over time (200 ms, 25-ms sliding window) between 500 ms prior and 1,500 ms after test probe onset (vertical hatched line). A cluster analysis revealed that *z*HFA during hits was significantly different from the other three trial types between 575 and 850 ms after test probe onset. Single and double asterisks denote significance, $P < 0.05$ and $P < 0.01$, respectively; see *Results* for full statistical reporting. (*B*) *z*HFA in the lateral temporal cortex during recognition. Analyses as above were carried out in the lateral temporal cortex. In this region, *z*HFA values did not significantly vary as a function of target–lure status or response choice, nor as an interaction between these two factors. Furthermore, there was no significant cluster wherein the four conditions varied over time ($P > 0.05$).

with each stimulus, thus maximizing true positives (hits) and minimizing false positives (false alarms).

Subjects completed one to five sessions (mean, 2.22) during which they endorsed 72% of targets and 41% of lures as old items, yielding a mean across-subject d' of 0.92 [$d' = z$(hit rate) – z(false alarm rate)]. As expected, reaction times were faster for items associated with stronger memory strength [hits, 1,361 ± 43 ms, vs. false alarms, 1,704 ± 57 ms; $t_{(65)} = 20.6$; $P < 0.001$].

Our neural analysis focused on the hippocampus; however, we included the lateral temporal cortex to control for brain-wide effects and the perirhinal cortex (PRC) given its well-established involvement in recognition memory (1). To achieve precise localizations, a neuroradiologist carefully reviewed each subject's computed tomography (CT) and MRI scans to determine the brain region in which each MTL electrode was located. In each brain region, subjects' electrodes numbered as follows: hippocampus, 26 (left, 6; right, 11; bilateral, 9); lateral temporal lobe, 66 (left, 14; right, 19; bilateral, 33); PRC, 23 (left, 9; right, 9; bilateral, 5). Fig. S1*B* illustrates a representative subject's MTL electrode coverage.

We compared *z*HFA across target–lure status and old–new choice. To ensure subjects were engaged in the task, we limited our first analysis to sessions in which behavioral performance exceeded a d' value of 0.50, leaving a total of 22 subjects (out of 26 with hippocampal recordings) with at least one adjacent pair of hippocampal electrodes. We focused on *z*HFA power between 200 and 1,000 ms following test word presentation given the latency between the item presentation and information flow from the visual cortex to the MTL via the ventral visual stream (32).

We found that, although *z*HFA in the hippocampus did not differ across target–lure status [two-factor, repeated-measures ANOVA; main effect, target vs. lure: $F_{(1,21)} = 2.57$, mean squared error (MSE) = 0.021, $P = 0.114$] nor across response choice [main effect, old vs. new: $F_{(1,21)} = 2.22$, MSE = 0.018, $P = 0.142$], alone there was a significant interaction between these factors [$F_{(1,21)} = 5.05$, MSE = 0.040, $P = 0.028$; Fig. 1*A*, *Left*]. In other words, hippocampal HFA differed between previously viewed compared with novel stimuli, but only when accounting for the response choice that was given. Post hoc paired t tests revealed that *z*HFA associated with hit (previously viewed stimuli, old response choice) trials was greater than the other three types of trials [vs. miss, false alarm, and correct rejection, all $P < 0.05$; comparisons remained significant following false-discovery rate corrections ($q = 0.10$)] (33). We excluded the possibility that recency confounded the finding of a *z*HFA dissociation, e.g., words with shorter study–test lags may have been recognized more often and associated with greater hippocampal activation, by showing a an absence of a recency effect in our data (Fig. S2). Neither the temporal lobe (Fig. 1*B*, *Left*) nor perirhinal *z*HFA values demonstrated significant main effects or interaction terms when the data were tested with analogous two-factor (target–lure status, response choice) ANOVA tests (all $P > 0.05$).

We next leveraged the favorable temporal properties of *z*HFA (Fig. 1*A*, *Right*). Using a temporal clustering procedure (34) to control the type-I error rate, hit *z*HFA in the hippocampus differed from miss, false alarm, and correct rejection *z*HFA between 575 and 850 ms (permutation procedure, $P = 0.003$; shaded region, Fig. 1*A*). We did not identify any significant temporal clusters of *z*HFA dissociation in lateral temporal lobe (Fig. 1*B*, *Right*) or PRC.

If hippocampal HFA is truly a biomarker of effective recognition, then one might expect that subjects who exhibit stronger activations during hit trials would also exhibit superior memory performance overall. To assess this prediction, we measured the relationship between each subject's recognition performance (d') and his/her *z*HFA power between 575 and 850 ms following the onset of test items during hit trials. We found a strong, positive correlation between *z*HFA and memory performance in the hippocampus [$r_{(25)} = 0.56$, $P = 0.003$; Fig. 2]. We did not identify a significant correlation when examining these relationships in the lateral temporal lobe [$r_{(65)} = -0.09$, $P = 0.47$] or in the PRC [$r_{(22)} = 0.24$, $P = 0.27$]; nota bene: this analysis includes all subjects with electrodes in each brain region because we did not apply the behavioral criteria $d' > 0.5$ to assess the full range of performance variability. An across-subject regression model of the form $\mathbf{d} = \beta_0 + \beta_H\mathbf{h} + \beta_M\mathbf{m} + \beta_{FA}\mathbf{f} + \beta_{CR}\mathbf{c}$, where **d** was a vector of each subject's d' value and **h**, **m**, **f**, and **c** were vectors of each subject's average *z*HFA for each type of trial (hit, miss, false alarm, correct rejection) demonstrated that hippocampal *z*HFA power associated with hit trials independently accounted for the

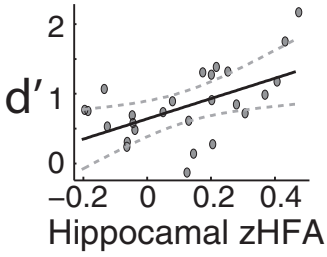

Fig. 2. Across-subject recognition memory–HFA correlation in the hippocampus. Recognition performance (d') and the hippocampal *z*HFA during successful response choices to previously viewed items (hit trials) positively correlated. Each dot represents a subject's *z*HFA power between 575 and 850 ms following word onset and his/her behavioral performance as measured by d'. The line of best fit (solid) and 95% confidence intervals (hatched) are shown.

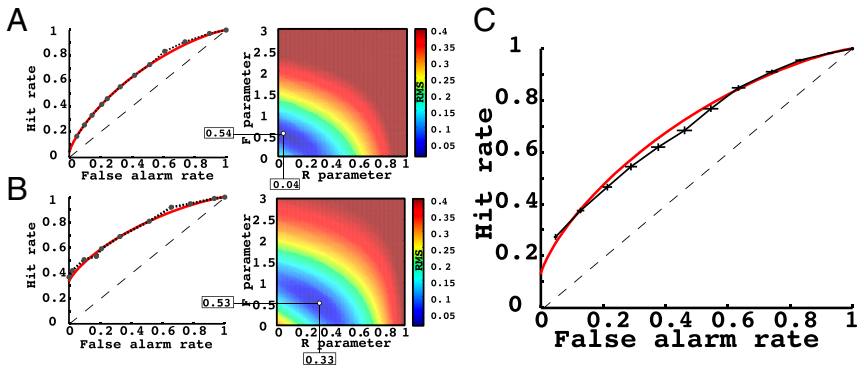

Fig. 3. (*A*) Example model fit for one subject: low recollection. (*Left*) The best-fitting model (red line) was fit to the subject's ROC curve, derived using response latency data (black dashed line). (*Right*) The root-mean-square deviation (RMSD) values for all model fits in the grid search for this subject are shown. The best-fitting model in the left panel corresponded to the lowest RMSD pixel in the right panel. This subject has a very low recollection parameter, as indicated on the plot. (*B*) Example model fit for one subject: high recollection. Identical plot as in Fig. 3*A* for a subject with a strong recollection pattern of recognition. (*C*) Final across-subject behavioral and model-based ROC. The ROC plot across all subjects is shown for the behavioral data (black dashed line) as well as the model fits (red line). Error bars correspond to the SEM across all subjects.

variability in recognition performance [normalized $\beta_H = 0.57, t_{(21)} = 2.47, P = 0.013$; all other values of $P > 0.1$]. Response choice-locked analyses (Figs. S3 and S4) underscored that the behavioral–neural correlation was not based on motor execution.

We next implemented a behavioral model of memory to obtain more specific and psychologically meaningful metrics of recognition memory performance. We chose the dual-process signal detection model (DPSM) of recognition memory because of its simplicity and widespread application (1, 4, 12, 17, 18, 35), and to answer a key question of recognition memory: is hippocampal activity specific to recollection (2, 36), or does it correspond to both the recollection and familiarity processes (4, 25)?

Because we did not collect confidence–judgment data, we used response latency as a surrogate for confidence, based on extensive prior work showing that subjects respond more quickly when they are confident in the accuracy of their response (37). In Fig. 3 *A* and *B*, we provide two representative subject examples of the actual receiver operating characteristic (ROC) curves fit using response latency data binned into six "confidence levels" (black dashed line), as well as the ROC from the best DPSM fit (red line). In the right panel of each figure, we also show the entire grid search for all possible model fits and display the best-fitting model with projections down to the *x* axis (recollection model parameter, *R*) and the *y* axis (familiarity model parameter, *F*; see *Supporting Information* for model details). From the figure, the subject in Fig. 3*A* has a very symmetric ROC function and, accordingly, the best-fitting model parameter estimate for recollection was relatively low ($R = 0.04$). In contrast, the subject in Fig. 3*B* has an asymmetric ROC curve, resulting in a much higher recollection model parameter estimate ($R = 0.33$). The latter subject likely performs recognition by recollecting the episodic details along with items at a much higher rate [see Fig. S5 for each subject's parameter (*R*,*F*) estimates]. The average (SEM) *R* parameter was 0.129 (0.016) and the average *F* parameter was 0.576 (0.045). Average behavioral and model ROC curves are shown in Fig. 3*C*.

To assess whether the strength of the recollection and familiarity processes tracked hippocampal activation, we correlated the functionally relevant signal we describe above (*z*HFA between 575 and 850 ms during hit trials) with the *R* and *F* parameters across all subjects with electrodes in this region. We found significant correlations between each of these latent cognitive variables and our neuronal measure of activation in the hippocampus [*R*: $r_{(25)} = 0.54, P = 0.004$; *F*: $r_{(25)} = 0.48, P = 0.012$; Fig. 4]. To assess the independent variability in hippocampal *z*HFA that each of these processes explained, we applied the following linear regression model: $\mathbf{h} = \beta_0 + \beta_R\mathbf{r} + \beta_F\mathbf{f}$, where $\mathbf{h}$ was a vector of the average *z*HFA values in the hippocampus during the time interval we identified above (575–850 ms) for each subject, and $\mathbf{r}$ and $\mathbf{f}$ were vectors containing the respective parameter estimates for each subject. We found that *R* positively correlated with *z*HFA in the hippocampus [$\beta_R = 0.63, t_{(23)} = 2.41$, and $P = 0.024$] and that *F* strongly trended in the same direction [$\beta_F = 0.20, t_{(23)} = 1.85$, and $P = 0.077$]. These results indicate that hippocampal activity reflects both the recollection and familiarity processes within dual-process theories of recognition memory. Our findings may also be explained by univariate models of recognition memory (38), as hippocampal activity closely tracked d' (Fig. 2).

Discussion

Our results indicate that hippocampal HFA dissociates based on integration of stimulus evidence (true target–lure status) and subject response choice (old, new). This marker of neuronal activity is greater during hits compared with other trial types, and strongest

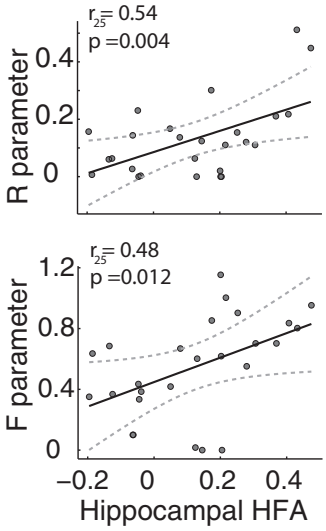

Fig. 4. Hippocampal HFA correlation with recollection and familiarity parameter estimates. Both recollection and familiarity parameter estimates correlated with hippocampal *z*HFA. Each dot represents a subject's average *z*HFA power between 575 and 850 ms following word onset during hit trials and his/her parameter estimate as determined by the dual-process model fit. The line of best fit (solid) and 95% confidence intervals (hatched) are shown.

between 575 and 850 ms after test item display. The functional relevance of this signal to recognition memory was supported by the correlation between the magnitude of hippocampal HFA and overall recognition performance across subjects. Such HFA dissociations and HFA–performance correlations were not found in the lateral temporal lobe or PRC. Both recollection and familiarity components of recognition correlated with hippocampal activity, addressing a long-standing question whether hippocampal computations are specific to recollection only.

Activity from the MTL sites has been linked to several types of signals, e.g., recency, novelty, and familiarity, composing recognition memory (39). In search of these signals, recognition memory studies vary widely in choice of experimental comparison (21). Instead of an a priori choice, we incorporated data from all electrodes and all trials, and assessed whether hippocampal HFA varies based on the two main factors in recognition: true target–lure status and subject response choice. Indeed, we found that both target–lure status and response choice are represented in the hippocampus. A dissociation of recognition memory signals between 575 and 850 ms accords well with peristimulus histograms of single-unit recordings in humans (e.g., refs. 40) and in behavior as it precedes the motor response. Moreover, a neural signal 275 ms in duration is likely blurred by measurements with less fine time resolution such as fMRI.

The DPSM (11, 12) has been widely used to study recognition memory (e.g., refs. 2, 4, 17, 18, 25, 36, 41, and 42) and assumes that recognition is based on two independent processes: familiarity, or a general sense of knowing, and recollection, characterized by reinstatement of episodic contextual details. ROC functions are a common method of estimating the contributions of recollection and familiarity to recognition memory (e.g., ref. 43). Although ROC curves are typically based on confidence judgements, response latencies inversely correlate with memory strength and provide a similar internal representation of response bias to generate ROC curves (44–46). Assuming that the DPSM provides valid estimates of recollection and familiarity, our finding that hippocampal HFA correlates with both parameters across subjects strongly suggests that computations in this structure support both processes (consistent with refs. 4 and 25) and rejects theories in which the hippocampus only subserves recollection (2, 47).

Our results are also consistent with more parsimonious models of recognition memory, e.g., the unequal variance signal detection model. Such theories do not posit independent cognitive variables that generate a recognition decision, but rather conceptualize memory strength as an integration of many sources of evidence, including familiarity and recollection (38). That the relative HFA values of the four trial types in Fig. 1*A* (*Left*) are generally consistent with memory strength (a summed representation of the many dimensions of memory) and memory reinstatement (37), and that HFA correlated with both overall and specific measures of recognition (Figs. 2 and 4) support such univariate signal detection theories. Although our analyses are model dependent and different decompositions of recognition memory could lead to different results, two classic models of recognition memory (the DPSM and signal detection theory) lead to the conclusion that the hippocampus plays a crucial role in recognition processes.

Although data from lesion, fMRI, and other electrophysiological measures are invaluable, their shortcomings may explain the discrepant results and common absence of a correlation to performance. The extent of lesions in patients is uncontrolled. Furthermore, in these types of studies, researchers cannot isolate processes of the memory system, such as encoding or recognition, but rather determine what tissue is necessary for a given function. fMRI suffers from variable hemodynamic transfer functions and, in the MTL, unpredictable signal dropout (21). Moreover, the temporal resolution of this modality is inferior compared with more direct neural measures. With regard to electrophysiology signals, the event-related potential suffers from issues such as polarity and excessive averaging across time (30), and neuronal spiking (from microwires) samples from an extremely small volume of tissue (48).

Intracranial HFA overcomes many of these shortcomings. HFA can be thought of as an activation signal that measures the overall firing rate of many thousands of neurons at the mesoscopic level (30, 31, 49) and intracranial HFA recorded from a macroelectrode can be interpreted very similarly as multiunit activity recorded by a microelectrode, albeit on a different spatial scale. In a recent study of recognition memory, Wixted et al. (29) demonstrated that hippocampal single-unit and multiunit recordings contain information pertaining to stimulus evidence (true target–lure status, irrespective of response choice). Both this study and ours show that hippocampal neuronal activity tracks d'. The results we report demonstrate that when neuronal activity is summed from a larger volume, hippocampal computations also reflect remembering or forgetting, i.e., subject response choice, and both the recollection and familiarity processes.

Our results provide necessary neural–behavioral and timing information to design causal studies, for example, direct hippocampal stimulation, aimed at augmenting memory. In one possible design, low HFA from the hippocampus would indicate a low likelihood of recognition and trigger a stimulation pulse intended to alter a "poor recognition state." Alternatively, future studies should determine whether boosting hippocampal HFA during recognition improves memory performance. Our findings indicate that modulations of hippocampal HFA may affect both recollection and familiarity, which will be used to inform such analyses in the context of neurocognitive models. However, another potential application of these findings is a prediction of postoperative memory decline following hippocampectomy for epilepsy treatment. In this case, the magnitude of the hippocampal HFA increase for successful recognition could be used to anticipate the risk of memory decline with resection (for support of such application within the parahippocampal gyrus, see ref. 50).

Conclusions

In sum, we report the precise time course of a neuronal dissociation based on both true target–lure status and response choice in the hippocampus during recognition memory. Not only did HFA dissociate, the magnitude of neuronal activity predicted variability in performance across subjects and tracked the degree to which subjects used recollection and familiarity. Seen through the lens of dual-process theories of recognition, our model-based results rule out the possibility that recollection is specific and exclusive to the hippocampus, and thus address a long-standing debate among memory scholars.

Materials and Methods

Subjects, Recognition Task, and Power Computation. Patients with medication-resistant epilepsy underwent surgical procedures in which depth, strip, or grid intracranial electrodes were implanted to localize epileptogenic regions for possible surgical resection. Data were collected over a 9-y period as part of a multicenter collaboration. Our research protocol was approved by the institutional review board at each hospital (Hospital of the University of Pennsylvania, Philadelphia; Freiburg University Hospital, Freiburg, Germany; and Thomas Jefferson University Hospitals, Philadelphia), and informed consent was obtained from the subjects. Our subject pool consisted of 66 left-language–dominant patients with at least two (to generate a bipolar montage) depth electrodes in the hippocampus ($n = 26$) or PRC ($n = 23$), or subdural electrodes in the lateral temporal lobe ($n = 66$). The placement of electrodes was strictly determined by clinical criteria. Each subject participated in an old–new recognition task of high-frequency nouns during a simultaneous intracranial electroencephalographic (iEEG) recording (Fig. S1*A*). We convolved segments of the iEEG signal with complex-valued Mortlet wavelets normalized to the 500 ms before test item onset, generating the *z*HFA signal (51). Please see *Supporting Information* for more details.

Statistical Procedures. In our item recognition task, there were four types of response choices based on the test item (stimulus) and subject response choice: true positives (hits), true negatives (correct rejections), false positives (false alarms), and false negatives (misses). Within each brain region, we compared the *z*HFA power associated with each of the possible stimulus evidence (target, lure) and response choice (old, new) combinations. For each subject's sessions, a normalized power value was calculated for the 200- to 1,000-ms time epoch relative to onset of the test item. For all sessions and electrodes for each subject, we assessed whether *z*HFA power varied as a function of stimulus type, response choice, or an interaction of these factors with a repeated-measures, two-factor ANOVA. When significant, we assessed for *z*HFA power differences among each of the four trial types with post hoc paired *t* tests and applied a false-discovery procedure ($q = 0.10$) (33) to control our false-positive rate. We further explored the timing dynamics of the *z*HFA difference using a cluster-based permutation procedure to identify contiguous time bins that distinguished among the four stimulus evidence–response choice combinations while controlling for type-I error (34). In regions showing significant differences among hit, correct rejection, false alarm, and miss *z*HFA power values, we assessed the Pearson correlation coefficient between *z*HFA power at latencies determined by the aforementioned timing analysis and memory performance as indexed by d'. We performed an analogous correlation analysis between *z*HFA power and our behavioral modeling parameter estimates (see below).

Behavioral Modeling. To model each subject's memory performance, we used a dual-process model of recognition memory (the DPSM) (35). The model compares a decision variable to a response criterion, thus generating a response choice (OLD or NEW). Recollection, which is independent of the response criterion, and familiarity, which is drawn from a normal distribution, compose OLD response choices. Confidence judgements, which are typically used to estimate response criteria, were abandoned to simplify the task in the in-patient hospital setting. Given the well-documented, inverse relationship between memory strength (more broadly, signal detection) and reaction time (44, 52) (e.g., reaction time for hits was much faster than false alarms in our experiment; see *Results*), we used response latency to approximate response criteria when making the empirical ROC curves (45, 46). By applying the model to each patient's behavioral data, we generated recollection and familiarity estimates for each subject. For further details of our behavioral modeling, see *Supporting Information*.

Data Sharing. All behavioral, electrophysiological, and localization-related data analyzed in this report are freely available at M.J.K.'s website (memory.psych.upenn.edu/Main_Page).

ACKNOWLEDGMENTS. We thank Dale H. Wyeth and Edmund Wyeth for technical assistance; Erin N. Beck for data collection; and Ashwin Ramayya, Nicole Long, M. Karl Healey, and Youssef Ezzyat for helpful discussion and input. We also thank members of the clinical teams where the data were collected: Ashwini Sharan, James Evans, Michael Sperling, Timothy Lucas, and Gordon Baltuch. We are indebted to the patients who have selflessly volunteered their time to participate in our study. This work was supported by National Institutes of Health Grant MH055687.

1. Eichenbaum H, Yonelinas AP, Ranganath C (2007) The medial temporal lobe and recognition memory. *Annu Rev Neurosci* 30:123–152.
2. Sauvage MM, Fortin NJ, Owens CB, Yonelinas AP, Eichenbaum H (2008) Recognition memory: Opposite effects of hippocampal damage on recollection and familiarity. *Nat Neurosci* 11(1):16–18.
3. Wixted JT, Squire LR (2011) The medial temporal lobe and the attributes of memory. *Trends Cogn Sci* 15(5):210–217.
4. Dede AJ, Wixted JT, Hopkins RO, Squire LR (2013) Hippocampal damage impairs recognition memory broadly, affecting both parameters in two prominent models of memory. *Proc Natl Acad Sci USA* 110(16):6577–6582.
5. Aggleton JP, Shaw C (1996) Amnesia and recognition memory: A re-analysis of psychometric data. *Neuropsychologia* 34(1):51–62.
6. Murray EA, Mishkin M (1998) Object recognition and location memory in monkeys with excitotoxic lesions of the amygdala and hippocampus. *J Neurosci* 18(16): 6568–6582.
7. Duva CA, et al. (1997) Disruption of spatial but not object-recognition memory by neurotoxic lesions of the dorsal hippocampus in rats. *Behav Neurosci* 111(6):1184–1196.
8. Manns JR, Hopkins RO, Reed JM, Kitchener EG, Squire LR (2003) Recognition memory and the human hippocampus. *Neuron* 37(1):171–180.
9. Zola SM, et al. (2000) Impaired recognition memory in monkeys after damage limited to the hippocampal region. *J Neurosci* 20(1):451–463.
10. Clark RE, Zola SM, Squire LR (2000) Impaired recognition memory in rats after damage to the hippocampus. *J Neurosci* 20(23):8853–8860.
11. Mandler G (1980) Recognizing: The judgment of previous occurrence. *Psychol Rev* 87(3):252–271.
12. Yonelinas AP (2002) The nature of recollection and familiarity: A review of 30 years of research. *J Mem Lang* 46(3):441–517.
13. Eichenbaum H, Sauvage M, Fortin N, Komorowski R, Lipton P (2012) Towards a functional organization of episodic memory in the medial temporal lobe. *Neurosci Biobehav Rev* 36(7):1597–1608.
14. Brown MW, Aggleton JP (2001) Recognition memory: What are the roles of the perirhinal cortex and hippocampus? *Nat Rev Neurosci* 2(1):51–61.
15. Schacter DL, Alpert NM, Savage CR, Rauch SL, Albert MS (1996) Conscious recollection and the human hippocampal formation: Evidence from positron emission tomography. *Proc Natl Acad Sci USA* 93(1):321–325.
16. Yonelinas AP, et al. (2002) Effects of extensive temporal lobe damage or mild hypoxia on recollection and familiarity. *Nat Neurosci* 5(11):1236–1241.
17. Fortin NJ, Wright SP, Eichenbaum H (2004) Recollection-like memory retrieval in rats is dependent on the hippocampus. *Nature* 431(7005):188–191.
18. Diana RA, Yonelinas AP, Ranganath C (2010) Medial temporal lobe activity during source retrieval reflects information type, not memory strength. *J Cogn Neurosci* 22(8):1808–1818.
19. Wais PE, Wixted JT, Hopkins RO, Squire LR (2006) The hippocampus supports both the recollection and the familiarity components of recognition memory. *Neuron* 49(3): 459–466.
20. Kirwan CB, Wixted JT, Squire LR (2010) A demonstration that the hippocampus supports both recollection and familiarity. *Proc Natl Acad Sci USA* 107(1):344–348.
21. Henson R (2005) A mini-review of fMRI studies of human medial temporal lobe activity associated with recognition memory. *Q J Exp Psychol B* 58(3-4):340–360.
22. Eldridge LL, Knowlton BJ, Furmanski CS, Bookheimer SY, Engel SA (2000) Remembering episodes: A selective role for the hippocampus during retrieval. *Nat Neurosci* 3(11):1149–1152.
23. Vilberg KL, Rugg MD (2007) Dissociation of the neural correlates of recognition memory according to familiarity, recollection, and amount of recollected information. *Neuropsychologia* 45(10):2216–2225.
24. Staresina BP, Fell J, Do Lam AT, Axmacher N, Henson RN (2012) Memory signals are temporally dissociated in and across human hippocampus and perirhinal cortex. *Nat Neurosci* 15(8):1167–1173.
25. Wais PE, Squire LR, Wixted JT (2010) In search of recollection and familiarity signals in the hippocampus. *J Cogn Neurosci* 22(1):109–123.
26. Smith ME, Stapleton JM, Halgren E (1986) Human medial temporal lobe potentials evoked in memory and language tasks. *Electroencephalogr Clin Neurophysiol* 63(2): 145–159.
27. Rutishauser U, Schuman EM, Mamelak AN (2008) Activity of human hippocampal and amygdala neurons during retrieval of declarative memories. *Proc Natl Acad Sci USA* 105(1):329–334.
28. Jutras MJ, Buffalo EA (2010) Recognition memory signals in the macaque hippocampus. *Proc Natl Acad Sci USA* 107(1):401–406.
29. Wixted JT, et al. (2014) Sparse and distributed coding of episodic memory in neurons of the human hippocampus. *Proc Natl Acad Sci USA* 111(26):9621–9626.
30. Lachaux JP, Axmacher N, Mormann F, Halgren E, Crone NE (2012) High-frequency neural activity and human cognition: Past, present and possible future of intracranial EEG research. *Prog Neurobiol* 98(3):279–301.
31. Burke JF, Ramayya AG, Kahana MJ (2015) Human intracranial high-frequency activity during memory processing: Neural oscillations or stochastic volatility? *Curr Opin Neurobiol* 31:104–110.
32. Viskontas IV, Knowlton BJ, Steinmetz PN, Fried I (2006) Differences in mnemonic processing by neurons in the human hippocampus and parahippocampal regions. *J Cogn Neurosci* 18(10):1654–1662.
33. Benjamini Y, Hochberg Y (1995) Controlling the false discovery rate: A practical and powerful approach to multiple testing. *J R Stat Soc Ser B* 57:289–300.
34. Maris E, Oostenveld R (2007) Nonparametric statistical testing of EEG- and MEG-data. *J Neurosci Methods* 164(1):177–190.
35. Yonelinas AP (1994) Receiver-operating characteristics in recognition memory: Evidence for a dual-process model. *J Exp Psychol Learn Mem Cogn* 20(6):1341–1354.
36. Diana RA, Reder LM, Arndt J, Park H (2006) Models of recognition: A review of arguments in favor of a dual-process account. *Psychon Bull Rev* 13(1):1–21.
37. Kahana MJ (2012) *Foundations of Human Memory* (Oxford Univ Press, New York).
38. Wixted JT (2007) Dual-process theory and signal-detection theory of recognition memory. *Psychol Rev* 114(1):152–176.
39. Yassa MA, Stark CE (2008) Multiple signals of recognition memory in the medial temporal lobe. *Hippocampus* 18(9):945–954.
40. Fried I, Cameron KA, Yashar S, Fong R, Morrow JW (2002) Inhibitory and excitatory responses of single neurons in the human medial temporal lobe during recognition of faces and objects. *Cereb Cortex* 12(6):575–584.
41. Yonelinas AP, Otten LJ, Shaw KN, Rugg MD (2005) Separating the brain regions involved in recollection and familiarity in recognition memory. *J Neurosci* 25(11): 3002–3008.
42. Wixted JT, Mickes L, Squire LR (2010) Measuring recollection and familiarity in the medial temporal lobe. *Hippocampus* 20(11):1195–1205.
43. Yonelinas AP, Parks CM (2007) Receiver operating characteristics (ROCs) in recognition memory: A review. *Psychol Bull* 133(5):800–832.
44. Ratcliff R, Starns JJ (2009) Modeling confidence and response time in recognition memory. *Psychol Rev* 116(1):59–83.

45. Emmerich D, Gray J, Watson C, Tanis D (1972) Response latency, confidence, and rocs in auditory signal detection. *Percept Psychophys* 11(1):65–72.
46. Kahana MJ, Loftus G (1991) Response time versus accuracy in human memory. *The Nature of Cognition*, ed Sternberg RJ (MIT Press, Cambridge, MA), pp 322–384.
47. Yonelinas AP, Jacoby LL (2012) The process-dissociation approach two decades later: Convergence, boundary conditions, and new directions. *Mem Cognit* 40(5):663–680.
48. Buzsáki G, Anastassiou CA, Koch C (2012) The origin of extracellular fields and currents—EEG, ECoG, LFP and spikes. *Nat Rev Neurosci* 13(6):407–420.
49. Chang EF (2015) Towards large-scale, human-based, mesoscopic neurotechnologies. *Neuron* 86(1):68–78.
50. Kunii N, Kawai K, Kamada K, Ota T, Saito N (2014) The significance of parahippocampal high gamma activity for memory preservation in surgical treatment of atypical temporal lobe epilepsy. *Epilepsia* 55(10):1594–1601.
51. Addison PS (2002) *The Illustrated Wavelet Transform Handbook: Introductory Theory and Applications in Science, Engineering, Medicine and Finance* (Institute of Physics Publishing, Bristol, UK).
52. Carterette EC, Friedman MP, Cosmides R (1965) Reaction-time distributions in the detection of weak signals in noise. *J Acoust Soc Am* 38(4):531–542.
53. Merkow MB, Burke JF, Stein JM, Kahana MJ (2014) Prestimulus theta in the human hippocampus predicts subsequent recognition but not recall. *Hippocampus* 24(12): 1562–1569.
54. Geller AS, Schlefer IK, Sederberg PB, Jacobs J, Kahana MJ (2007) PyEPL: A cross-platform experiment-programming library. *Behav Res Methods* 39(4):950–958.
55. Burke JF, et al. (2013) Synchronous and asynchronous theta and gamma activity during episodic memory formation. *J Neurosci* 33(1):292–304.
56. Insausti R, et al. (1998) MR volumetric analysis of the human entorhinal, perirhinal, and temporopolar cortices. *AJNR Am J Neuroradiol* 19(4):659–671.
57. Onyper SV, Zhang YX, Howard MW (2010) Some-or-none recollection: Evidence from item and source memory. *J Exp Psychol Gen* 139(2):341–364.
58. Murdock BB, Kahana MJ (1993) List-strength and list-length effects: Reply to Shiffrin, Ratcliff, Murnane, and Nobel (1993). *J Exp Psychol Learn Mem Cogn* 19(6): 1450–1453.
59. Murdock BB, Anderson RE (1975) Encoding, storage, and retrieval of item information. *Information Processing and Cognition: The Loyola Symposium*, ed Solso RL (Erlbaum, Hillsdale, NJ), pp 145–194.

Supporting Information

Merkow et al. 10.1073/pnas.1513145112

SI Materials and Methods

Subjects. We defined language dominance as right-handedness or evidence of left-language dominance on intracarotid sodium amytal injection or fMRI testing. A subset of these subjects have been reported previously (e.g., ref. 53); however, unlike these previous reports, which focused exclusively on free recall or encoding of items, the analyses reported here examine the recognition test portion of the experiment, which until now has not been described. All of the analyses and results included here are novel.

Recognition Task. The recognition task (Fig. S1*A*) was developed using the Python Experiment–Programming Library (PyEPL) (54) and administered at the subject's bedside using a laptop computer. A fixation cross presented in the center of the screen signaled the onset of each study list. Lists comprised 15 words chosen randomly and without replacement from a pool of high-frequency nouns (memory.psych.upenn.edu/WordPools). Following a series of between 10 and 15 lists of word presentation each followed by delayed free-recall (a minimum 20-s arithmetic distractor separated encoding from recall), subjects were given a final old–new recognition memory test (Fig. S1*A*), which is the focus of this report. The variation in the total list count reflected slight experimental modifications over the 9-y period in which these data were collected. Sixty targets were randomly chosen from the studied items and intermixed with 60 lure items chosen from the same word pool. Each of these 120 test items was then presented individually, and subjects were asked to make old–new judgments by pressing one of two buttons on a computer keyboard with their right (indicating old) or left (indicating new) index finger. Subjects were given a maximum of 5 s to respond to each probe item. Following a jittered interstimulus interval of 2,400–2,600 ms, the next probe item was then presented.

iEEG Recordings. Clinical circumstances alone determined electrode number and placement. Depth electrode contacts were spaced every 6 or 8 mm apart and subdural electrodes (grids and strips) were spaced every 10 mm apart. iEEG was recorded using a DeltaMed (Natus), Nicolet, Grass Telefactor, or Nihon-Kohden EEG system. Sampling rates ranged from 400 to 2,000 Hz. Signals were converted to a bipolar montage by differencing the recordings between each pair of immediately adjacent contacts on grid, strip, and depth electrodes (55). Signals were then resampled at 400 Hz. Analog pulses (±5 V) were sent to the clinical amplifier from the experimental laptop to synchronize the electrophysiological recordings with behavioral events. Recordings were normalized within session to the 500 ms before test item onset, yielding the *z*HFA signal.

Brain Regions. A neuroradiologist experienced in neuroanatomical localization, but blinded to the electrophysiology data, manually reviewed postoperative CT and MRI images to localize depth electrodes within the medial temporal lobe (MTL). All bipolar pairs in which adjacent contacts were within the hippocampus were included in the hippocampal region. All bipolar contacts with at least one electrode abutting the collateral sulcus (both in the parahippocampal and fusiform gyri) up to 1.5 cm posterior to the ventral margin of the hippocampal head were grouped into the perirhinal cortex (PRC) region (56). To ensure the neural activity in the MTL was not generalized to other brain regions, we also analyzed bipolar pairs of subdural electrodes from the lateral temporal lobe (lateral to the collateral sulcus). These electrodes were localized by coregistering the postoperative CTs with MRIs using FSL Brain Extraction Tool (BET) and FLIRT software packages. The resulting contact locations were mapped to both Montreal Neurological Institute and Talairach space using an indirect stereotactic technique to identify temporal lobe electrodes based on a standardized brain parcellation (55).

Cluster-Based Permutation Procedure. We used a cluster-based permutation procedure (34) to investigate the timing dynamics of the *z*HFA difference among the four stimulus evidence (i.e., true target–lure status)–response choice combinations while controlling for type I error.We began by performing a series of ANOVA tests on the normalized power distributions at each time bin: 200-ms time windows every 25 ms between 500 ms before and 1,500 ms after the onset of test item presentation, yielding a total of 80 time windows—and thus 80 *P* values associated with each ANOVA test—surrounding word presentation for each subject. To normalize the distribution of these *P* values, we calculated a corresponding *z* value for each *P* value using the standard normal distribution. To test the reliability of these *z* values across subjects, we performed a series of one-sample *t* tests, one at each time bin, comparing the distribution of subjects' *z* values to zero. To correct for multiple comparisons, we identified the largest clusters of temporally adjacent windows where the four stimulus evidence–response choice combinations significantly varied from one another ($P < 0.05$ across participants) and computed the cluster statistic as the sum of *t* statistics across these windows (true cluster). We then estimated the false-positive rate for each of these cluster statistics using a permutation-based shuffle procedure. For each iteration of the procedure, we randomly changed the sign of the *t* statistics computed for each subject, and computed the cluster statistics associated with the largest contiguous significant increase observed in the shuffled data across subjects (null cluster). We repeated this procedure 10,000 times and estimated a distribution of null clusters, which reflect cluster statistics that would be obtained if power values did not reliably differ between the four trial types. We derived a *P* value for each cluster statistic based on where the true cluster fell on this null distribution.

Behavioral Modeling. To model each subject's memory performance, we used a dual-process model of recognition memory [the dual-process signal detection model (DPSM) (35)]. This model proposes that recognition is the output of a continuous decision variable that is compared with a response criterion, *c*. When the decision variable is greater than the response criterion the model responds "OLD"; when the evidence is below the response criterion, the model responds "NEW." In the DPSM, the lure decision variable is drawn from normal distribution, and the target decision variable has two components. For targets that are recognized by recollection, the model responds OLD independent of the response criteria. For targets that are recognized by familiarity, the decision variable is drawn from a normal distribution with a mean that is *F* SD units greater than that for the lures. Mathematically,

$$P(\text{“}OLD\text{”} \le k | OLDITEM) = R + (1-R)\Phi(c_k, -F/2, 1), \quad \textbf{[S1]}$$

$$P(\text{“}NEW\text{”} \le k | NEWITEM) = \Phi(c_k, -F/2, 1). \quad \textbf{[S2]}$$

The particular form of dual-process model was taken from ref. 57, where $\Phi(x, \mu, \sigma)$ represents a cumulative distribution function of

a normal distribution integrated at x with mean μ and SD σ. k represents the level of confidence of the response criteria, R reflects the proportion of items that are recollected, and F represents the amount (in SD) that the mean of the familiarity decision variable distribution is greater than the lure distribution (57).

To fit the model to the behavioral data for each subject, we calculated the hit rate (Eq. **S1**) and the false-alarm rate (Eq. **S2**) for many levels of response criteria, c_k, which yielded the receiver operating characteristic (ROC) curve (35). The area under this curve is proportional to recognition task performance, and the asymmetry of the curve reflects the degree of recollection during task performance (1). In this recognition paradigm, confidence judgements, which typically are used as a proxy for c_k, were abandoned to simplify the task in the in-patient hospital setting. As a result, we used response latency to approximate c_k when making the empirical ROC curves (45, 46). Next, we performed a grid search of the two DPSM parameters, R and F, to generate a set of model ROC curves for each subject. The parameters that minimized the root-mean-squared deviation of the model-based ROC and the empirical ROC were chosen.

SI Results

In each session there was an average (SD) of 43.3 (7.8) hits, 15.9 (7.6) misses, 25.2 (13.1) false alarms, and 34.3 (13.2) correct rejections. As expected, across-subjects response latencies were shorter for hits ($1{,}361 \pm 43$ ms) than for misses ($1{,}810 \pm 62$ ms), false alarms ($1{,}704 \pm 57$), and correct rejections ($1{,}648 \pm 61$) [ANOVA, $F_{(3,65)} = 45.3$; MSE $= 2.4 \times 10^3$; $P < 0.001$, and all P values associated with paired t stats <0.001].

Recognition memory exhibits a recency effect such that items with shorter delays between study and test are more often recognized (58). To rule out a possible confound of recency (e.g., zHFA may increase for words with shorter periods between study and test, and these words could be more likely recognized), we searched for the presence of a recency effect in the behavioral data. We examined performance as a function of study–test lag, defined as the number of cognitive events (word encodings, arithmetic distractors, word recalls, test items) between study and test (59). Fig. S2 shows the hit rate (probability of recognizing a studied word) as a function of lag quintile. A random-effects, one-way ANOVA demonstrated that performance did not significantly vary across the different lag groups [$F_{(4,334)} = 0.86$, mean squared error (MSE) = 0.009, $P = 0.490$]. The absence of a lag effect is likely the result of our experimental design, in which there is a substantial delay between study and test for all words.

To further ensure our item display-locked findings in the hippocampus were not the result of "bleed-in" from subject response choice, we conducted similar analyses to those in the main text (Figs. 1*A*, *Right*, and 2); however, in this case, hippocampal zHFA was aligned to the yes–no judgement (key press) rather than test item display. We identified a time interval preceding the response choice wherein the zHFA among trial types significantly varied and the zHFA associated with hits was greater than the other three stimulus–response choice combinations (225–50 ms; permutation procedure, $P = 0.023$; Fig. S3). However, the zHFA difference during this time interval did not correlate with d' [$r_{(25)} = 0.22, P = 0.272$; Fig. S4]. These results provided further evidence that the zHFA in the hippocampus was less likely related to motor execution, and more consistent with a memory signal.

As described in the main text, each subject's response latency data were used to generate recollection and familiarity estimates (Eq. **S1** and **S2**) by identifying the parameters that minimized the root-mean-squared deviation (RMSD) between the empirical and model ROC curves. Fig. S5 illustrates the average RMSD values for all subjects in parameter space and is superimposed on a scatterplot of the best model fits for all subjects ($n = 66$).

Using the area under the curve of the ROC as a proxy for performance, we found an average (SEM) of 0.685 (0.013) across all subjects, which was significantly better than the chance value of 0.5 [$t_{(65)} = 14.75, P < 0.001$]. The model provided a good fit to the behavioral data: the average RMSD values of the true ROC and the model ROC fits across subjects was 0.041 (0.021). The average R parameter was 0.129 (0.016) and the average F parameter was 0.576 (0.045). Average behavioral and model ROC curves are shown in Fig. 3*C*. In Fig. S5, we show the average of the RMSD fits across all subjects in parameter space, superimposed on the points of each subject's optimal model fit.

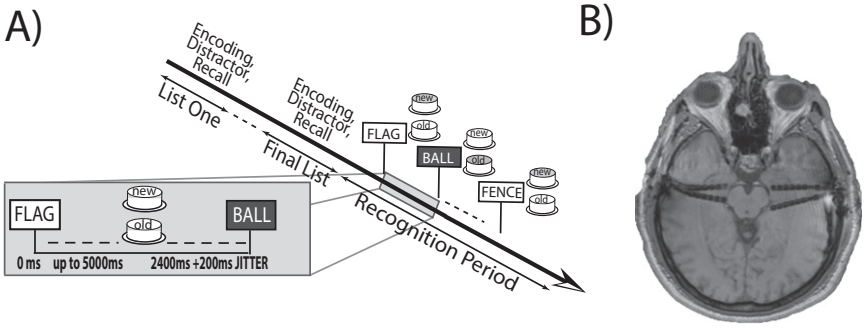

Fig. S1. (*A*) Recognition task. Subjects were shown a series of lists, each followed by delayed free recall. After all lists were completed, the subjects were shown shown 60 targets from the studied items and 60 lures, and asked to make a recognition judgment by button press with either the left (indicating new) or right (indicating old) index fingers. (*B*) MTL intracranial depth electrodes. Subjects underwent postimplantation MRIs, which were reviewed by a neuroradiologist for electrode localization purposes. In this example, the subject's recordings included both hippocampal and perirhinal contacts.

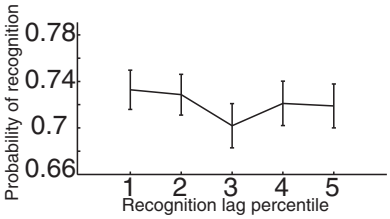

Fig. S2. Recency behavioral analysis. The number of cognitive events (word encodings, arithmetic distractors, word recalls, test items) between study and test (study–test lag) was calculated for each test item and binned into quintiles. Mean and ±1 SEM for hit rate as a function of study–test lag quintile are displayed; we did not find performance varied as a function of lag category [$F_{(4,334)} = 0.86$, mean squared error (MSE) = 0.009, $P = 0.490$].

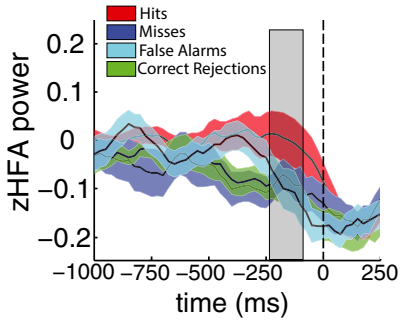

Fig. S3. Response choice-locked HFA power over time. Across-subject mean and ±1 SEM *z*HFA power for each of the four stimulus–response choice combinations (color schema same as in Fig. 1) over time (200 ms, 25-ms sliding window) between 1,000 ms prior and 250 ms after test item display (vertical hatched line). A cluster analysis revealed that *z*HFA significantly varies among the four conditions between 225 and 50 ms prior (shaded in gray) to test item display (permutation procedure, $P = 0.023$).

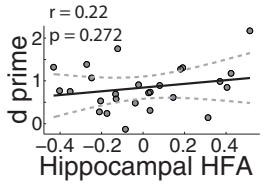

Fig. S4. Across-subject memory performance and response choice-locked hippocampal HFA correlation. No reliable relationship was found between recognition performance (d') and hippocampal *z*HFA during hit trials in the time interval identified in the previous, response choice-aligned analysis [$r_{(25)} = 0.22$, $P = 0.272$]. Each dot represents a subject's hippocampal *z*HFA power during successful recognition from 225 to 50 ms before response choice and his/her behavioral performance as measured by d'. The line of best fit (solid) and 95% confidence intervals (hatched) are shown.

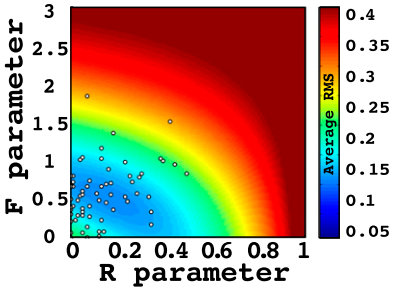

Fig. S5. Across-subject summary of model fits. The model fits (*R* and *F* parameters) for all subjects ($n = 66$) are shown as a scatter plot superimposed on the across-subject average RMSD values throughout parameter space. The average (SEM) *R* parameter across subjects was 0.129 (0.016), and the average *F* across subjects was 0.576 (0.045).